ORIGINAL ARTICLE

J Rhinol 2025;32(3):175-183 | https://doi.org/10.18787/jr.2025.00021 pISSN 1229-1498 / eISSN 2384-4361
www.j-rhinology.org

Optimizing Human Nasal Turbinate Stem Cell Dosage for the Effective Treatment of Empty Nose Syndrome

Yun Jin Kang, MD, PhD[1*], Dan Bi Park, PhD[2*], David W. Jang, MD[3], Mi Hyun Lim, PhD[2], Jae Yoon Lee, MD[4], Seung Yeon Yoo, MS[2], Sung Won Kim, MD, PhD[4], and Do Hyun Kim, MD, PhD[4]

[1]Department of Otolaryngology-Head and Neck Surgery, Yeouido Saint Mary's Hospital, College of Medicine, The Catholic University of Korea, Seoul, Republic of Korea
[2]Postech-Catholic Biomedical Engineering Institute, College of Medicine, The Catholic University of Korea, Seoul, Republic of Korea
[3]Department of Head and Neck Surgery & Communication Sciences, Duke University School of Medicine, Durham, NC, USA
[4]Department of Otolaryngology-Head and Neck Surgery, Seoul Saint Mary's Hospital, College of Medicine, The Catholic University of Korea, Seoul, Republic of Korea

Background and Objectives: Empty nose syndrome (ENS) is a chronic and debilitating condition characterized by atrophic nasal mucosa and impaired mucosal function, resulting in persistent nasal discomfort and breathing difficulties. Despite various surgical and medical interventions, an effective treatment remains elusive. This study investigated the therapeutic potential of a human nasal turbinate stem cell (hNTSC)-based therapeutic agent for ENS.

Methods: ENS was induced in a rabbit model via electrocautery, and varying concentrations of hNTSC-based spheroids combined with collagen hydrogel were administered (n=3 per group). Histological and mRNA expression analyses were performed one month post-treatment to assess epithelial thickness and *FOXJ1* expression levels.

Results: Histological analysis revealed that hNTSC treatment significantly increased epithelial thickness, with the most pronounced effect observed in the medium-dose group (1×10^7 cells/mL, 50 μL). mRNA analysis showed a dose-dependent increase in *FOXJ1* expression, with the highest levels observed in the high-dose group. However, this did not correlate with superior histological recovery, suggesting that epithelial remodeling is optimal at specific cell concentrations.

Conclusion: These findings demonstrate that hNTSC-based therapy effectively promotes epithelial regeneration in ENS, with an optimal therapeutic dose identified at 1×10^7 cells/mL. This study highlights the potential clinical application of stem cell therapy for ENS and underscores the need for precise dose optimization to maximize therapeutic outcomes.

Keywords: Empty nose syndrome; Stem cells; Nasal turbinates.

INTRODUCTION

Empty nose syndrome (ENS) is a chronic condition resulting from turbinate surgery, characterized by nasal dryness, impaired mucosal function, and paradoxical nasal obstruction, severely affecting patients' quality of life [1]. ENS is associated with paradoxical nasal obstruction despite an anatomically open nasal airway. Common symptoms experienced by ENS patients include nasal dryness, dyspnea, a sensation of suffocation, and impaired mucosal cooling, significantly impairing quality of life [2]. The pathophysiology of ENS is multifactorial, involving altered nasal aerodynamics, impaired mucosal thermoregulation, and disrupted neurosensory functions [3]. Surgical reduction of the inferior turbinates may result in diminished airflow resistance, disrupting normal nasal airflow patterns and reducing nasal mucosal stimulation [4]. Furthermore, reduced nasal airflow can impair the conditioning of inspired air, leading to mucosal desiccation and secondary inflammation [5]. Recent studies utilizing computational fluid dynamics have demonstrated abnormal airflow distribution and increased wall shear stress in ENS patients, further supporting the hypothesis that disrupted nasal airflow contributes to symptomatology [6]. Given its profound impact on

Received: April 5, 2025 **Revised:** May 13, 2025
Accepted: May 27, 2025

Address for correspondence: Do Hyun Kim, MD, PhD, Department of Otolaryngology-Head and Neck Surgery, Seoul St. Mary's Hospital, College of Medicine, The Catholic University of Korea, 222 Banpo-daero, Seocho-gu, Seoul 06591, Republic of Korea
Tel: +82-2-2258-6112, **Fax:** +82-2-535-1354, **E-mail:** dohyuni9292@naver.com
*These authors contributed equally to this work.

This is an Open Access article distributed under the terms of the Creative Commons Attribution Non-Commercial License (https://creativecommons.org/licenses/by-nc/4.0) which permits unrestricted non-commercial use, distribution, and reproduction in any medium, provided the original work is properly cited.

Copyright © 2025 Korean Rhinologic Society

respiratory function and overall well-being, ENS has gained increasing attention in rhinology, necessitating further research into its pathophysiology and treatment options.

Cell-based therapies have been explored for refractory diseases lacking effective treatment options, with promising results reported [7-9]. The therapeutic efficacy of cell-based therapies often significantly varies depending on the administered cell concentration. Published studies, particularly those involving mesenchymal stem cell-based therapies for osteoarthritis, have shown inconsistent results, with variations in cell dosage not always correlating with improved therapeutic outcomes. Indeed, higher concentrations sometimes resulted in reduced effectiveness [10,11]. Additionally, the form of cells and the integration of biomaterials in engineered therapeutic agents also critically influence their effectiveness [12]. Studies indicate that administering cells in spheroid form rather than as single cells enhances post-transplant cell viability, multipotency, and secretion of tissue-repairing factors [13,14]. Furthermore, engineering therapeutic agents by combining cells with biomaterials such as hydrogels has been associated with improved therapeutic efficacy and increased expression of stemness-related genes and proteins [15-17].

In this study, we aimed to develop a novel therapeutic approach for treating ENS, a condition currently lacking effective treatments. We established an ENS animal model and applied our cell-based therapeutic strategy to evaluate its efficacy. Our objective was to assess the effectiveness of these therapies and identify the optimal conditions to promote mucosal epithelium repair in ENS.

METHODS

Isolation and culture of human nasal turbinate stem cells

human nasal turbinate stem cells (hNTSCs) were isolated from nasal inferior turbinate tissue obtained from a healthy donor. Initially, the tissue was rinsed with gentamicin solution in the surgical suite, followed by washes with antibiotic-antimycotic solution (Gibco) and Dulbecco's phosphate-buffered saline (DPBS; Welgene). The tissue was then sectioned into 0.5 mm fragments and incubated at 37°C in Dulbecco's Modified Eagle Medium (Gibco), supplemented with 10% fetal bovine serum and Minimum Essential Medium-α (Gibco). The culture was maintained under 5% CO_2, sealed beneath a sterilized glass slide. After two weeks of cultivation, the cells were harvested and dissociated using TrypLE™ (Gibco). Cell morphology and concentration were assessed at 40× magnification (Fig. 1A).

Human nasal epithelial cells were obtained from a 38-year-old man diagnosed with allergic rhinitis undergoing elective nasal surgery. This research was performed at Seoul Saint Mary's Hospital with ethical approval from the Institutional Review Board of the Catholic University of Korea (Approval No. KC08TISS0341), and informed consent was obtained. All animal studies were approved by the Institutional Animal Care and Use Committee (IACUC) of the Catholic University of Korea (Approval No. CUMS-2024-0008-01).

Flow cytometry analysis

To characterize hNTSCs, cells were prepared as single-cell suspensions and incubated for one hour with phycoerythrin-labeled antibodies against mesenchymal stem cell markers, including CD14, CD34, CD73, CD90, and CD105 (BD Pharmingen). After incubation, cells were washed and resuspended in DPBS. Flow cytometry (BD FACSCanto II; Becton Dickinson) was conducted to evaluate cellular populations. hNTSCs were characterized by the absence of hematopoietic markers CD14 and CD34, alongside positive expression of mesenchymal markers CD73, CD90, and CD105.

Multi-lineage differentiation

The differentiation potential of hNTSCs into adipogenic, chondrogenic, and osteogenic lineages was assessed at passage 6 using differentiation media specific to each lineage (Gibco). Adipogenic differentiation was evaluated after two weeks by staining with Oil Red O (Sigma-Aldrich). Osteogenic differentiation was induced for three weeks and assessed using Alizarin Red staining (Sigma-Aldrich) to detect calcium deposition. For chondrogenic differentiation, spheroids were generated and stained with Alcian Blue (Abcam) after two weeks. All differentiation protocols followed the manufacturer's guidelines.

Preparation of the treatment agent

To formulate the therapeutic agent, hNTSCs were seeded overnight into StemFIT 3D® (MICROFIT) to form spheroids. These spheroids were then mixed with cold collagen type I hydrogel (COLTRIX® TendoRegen; Ubiosis) at varying cell concentrations. The therapeutic agent was administered in 50 μL aliquots using a 1 mL insulin syringe equipped with a 29-gauge needle (BD Pharmingen). For the vehicle control group, 50 μL of collagen hydrogel alone was administered to ensure consistency.

The dosing concentrations (2×10^6, 1×10^7, and 1×10^8 cells/mL) were selected based on previous findings demonstrating efficacy at 2×10^6 cells/mL in nasal epithelial regeneration [18]. Higher cell concentrations were included in this study to evaluate potential dose-dependent effects. Similar cell-dose ranges have shown therapeutic efficacy in other tissues, such as articular cartilage [19].

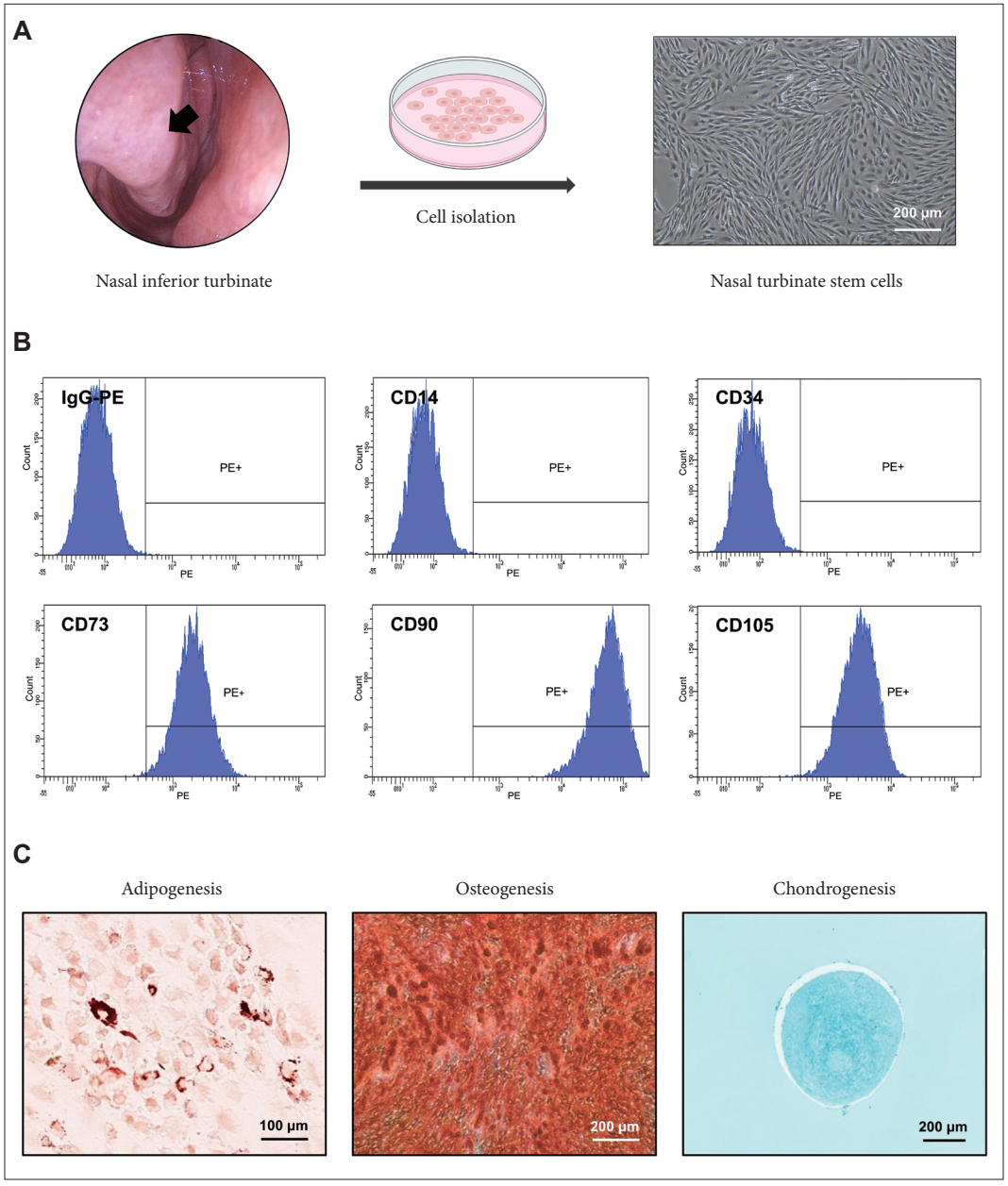

Fig. 1. Isolation, marker expression, and differentiation capabilities of hNTSCs. A: Endoscopic image showing the donor's inferior turbinate (arrow) and cultured hNTSCs isolated from turbinate tissue, visualized at 40×. B: Flow cytometry analysis confirming hNTSC surface markers, including IgG-PE, CD14, CD34, CD73, CD90, and CD105. C: hNTSCs differentiated into multiple lineages and stained for each marker. hNTSC, human nasal turbinate stem cell.

Cell viability analysis

Live and dead cells were identified using the LIVE/DEAD Viability/Cytotoxicity Kit (ThermoFisher Scientific). Cells were incubated for 30 minutes with the reagent and subsequently analyzed for cell viability using confocal laser microscopy (LSM 800; Carl Zeiss).

Surgical procedure in animal studies

Specific-pathogen-free New Zealand white rabbits (male, 3.0–3.5 kg) were obtained from Kangda. Rabbits were randomly divided into six experimental groups: sham (turbinate surgery only), vehicle (turbinate surgery with collagen hydrogel injection), three treatment groups (turbinate surgery with hNTSC application at three different doses), and normal control (no surgical intervention) (Table 1 and Fig. 2A).

Surgery involved making a midline incision approximately 3 cm from the nasal tip, followed by the removal of bilateral bone flaps (2.5×0.5 cm^2) using a micro-saw (Fig. 2B) [18]. The

electrocautery-based ENS model's reliability and reproducibility were previously validated [18]. Bone flaps were temporarily preserved in sterile saline, and turbinates were electrocauterized in all groups except the normal control. Immediately after electrocauterization, treatment agents were administered based on group allocation, and the bone flaps were repositioned. Rabbits in the treatment groups received 50 μL of hNTSC-based therapeutic agent, while those in the vehicle group received an equivalent volume of collagen hydrogel alone. Bone flaps were repositioned anatomically, and the skin and periosteal flaps were sutured. Four weeks after electrocauterization, tissue samples were collected for histological and molecular analysis.

All surgical procedures and tissue sampling were performed under standardized conditions by two expert rhinology specialists to ensure reproducibility and reliability. During the study, no severe adverse events or mortality occurred among the ENS-model rabbits.

Histological analysis

Tissue sections (4.0 μm thickness) were deparaffinized in xylene, rehydrated through graded ethanol solutions, and stained with Mayer's hematoxylin (Abcam) and eosin (Daejung, Korea). Additional sections were processed with Masson's trichrome (MT) staining according to the manufacturer's instructions (Abcam).

Table 1. Experimental group classification and treatment cell doses

Groups	Cell concentrations	n
Control	None	3
Sham	None	3
Vehicle	Only collagen hydrogel	3
Treatment		
Low	Collagen hydrogel + 2×10^6 cells/mL	3
Medium	Collagen hydrogel + 1×10^7 cells/mL	3
High	Collagen hydrogel + 1×10^8 cells/mL	3

RNA extraction and real-time quantitative polymerase chain reaction

Total RNA was extracted using TRIzol reagent (ThermoFisher Scientific). Reverse transcription was performed using the TOPscript RT DryMIX cDNA synthesis kit (Enzynomics, Korea). Quantitative polymerase chain reaction (PCR) was conducted using a CFX96 PCR detection system (Bio-Rad). Relative mRNA expression levels of acetylated α-tubulin were calculated using the $2^{-\Delta\Delta Ct}$ method, normalized to *HPRT1* as a reference control. Primer sequences used are listed in Table 2.

Quantitative and statistical analysis

The thickness of the pseudostratified epithelium was measured from randomly selected stained sections at 400× magnification. Regions of interest were defined, and pixel values were quantified using ImageJ software (ImageJ 1.54g; https://imagej.net/ij/). ImageJ was utilized to analyze pixel intensities corresponding to features of interest within the specified regions. Statistical analyses, including two-way ANOVA and the unpaired t-test, were performed using Prism 8.0 software (GraphPad Software).

RESULTS

Development of hNTSC-based therapeutic agent

The isolated hNTSCs were characterized by flow cytometry to confirm expression of specific surface markers. Hematopoietic stem cell markers CD14 and CD34 were negative,

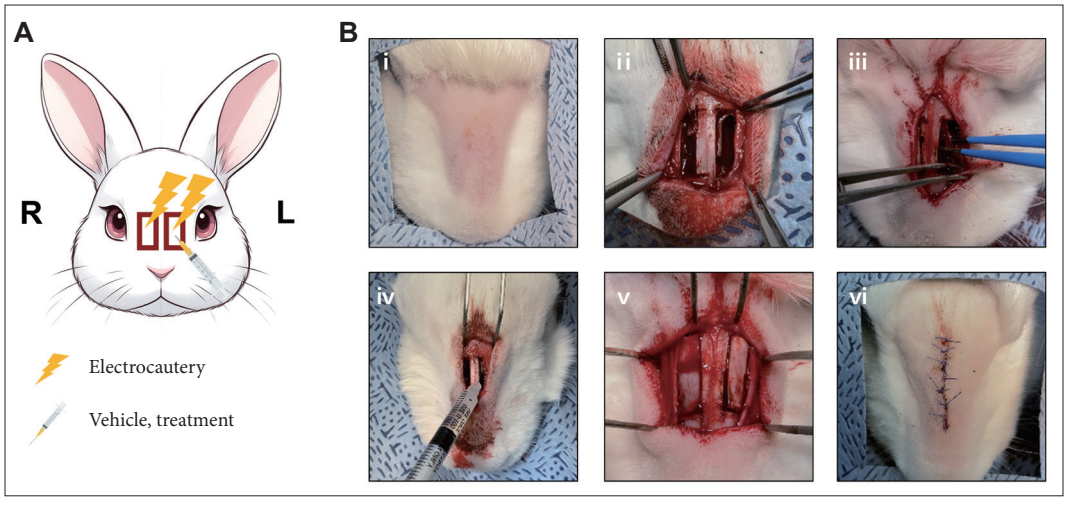

Fig. 2. Induction and treatment of ENS in the rabbit model. A: Overview of the induction of ENS and therapeutic agent administration in the rabbit model. B: Step-by-step process of ENS induction and treatment application in the rabbit model. ENS, empty nose syndrome.

whereas mesenchymal stem cell markers CD73, CD90, and CD105 were positively expressed, verifying the mesenchymal phenotype of the cells (Fig. 1B). Additionally, multi-lineage differentiation assays evaluated the differentiation potential of hNTSCs into adipogenic, osteogenic, and chondrogenic lineages. The hNTSCs successfully differentiated into all three lineages, demonstrating their robust adipogenic, osteogenic, and chondrogenic differentiation capacity (Fig. 1C).

To ensure uniform spheroid formation, hNTSCs were seeded into StemFIT 3D® and incubated overnight. The resulting spheroids were consistently sized, averaging 251.6±10.4 μm in diameter (Fig. 3A). These spheroids were then combined with collagen hydrogel to produce an injectable therapeutic agent (Fig. 3B). To assess the safety and viability of this spheroid-hydrogel mixture, Live/Dead staining was performed. The results indicated high cell viability, with live-cell percentages of 97.38%±0.4% in spheroids alone and 96.39%±3.06% after mixing with hydrogel (Fig. 3C and D).

Table 2. Primer sequences for RT-qPCR analysis

Gene	Primer	Sequence
HPRT1	Forward	GAC CAG TCA ACA GGG GAC AT
	Reverse	CTT GCG ACC TTG ACC ATC TT
α-SMA	Forward	GAG GCA CCA CTG AAC CCT AA
	Reverse	CAT CTC CAG AGT CCA GCA CA
FOXJ1	Forward	TCG ACT GGG AAG CCA TCT
	Reverse	GTC GAA GTC CAG GCT GTT G

RT-qPCR, real-time quantitative polymerase chain reaction; SMA, smooth muscle actin.

Induction of ENS and therapeutic agent administration in rabbit models

One month after surgery, histological and mRNA expression analyses confirmed successful ENS induction. Both hematoxylin and eosin (H&E) and Masson's trichrome staining revealed disrupted pseudostratified epithelial architecture in the sham group, characterized by epithelial atrophy, squamous metaplasia, and submucosal fibrosis (Fig. 4A and B). Quantification of epithelial thickness showed significant atrophy, with a 0.36±0.09-fold reduction compared to the control group (Fig. 4C). Furthermore, the area of submucosal fibrosis in the sham group increased approximately 4.73-fold, from 13.28%±

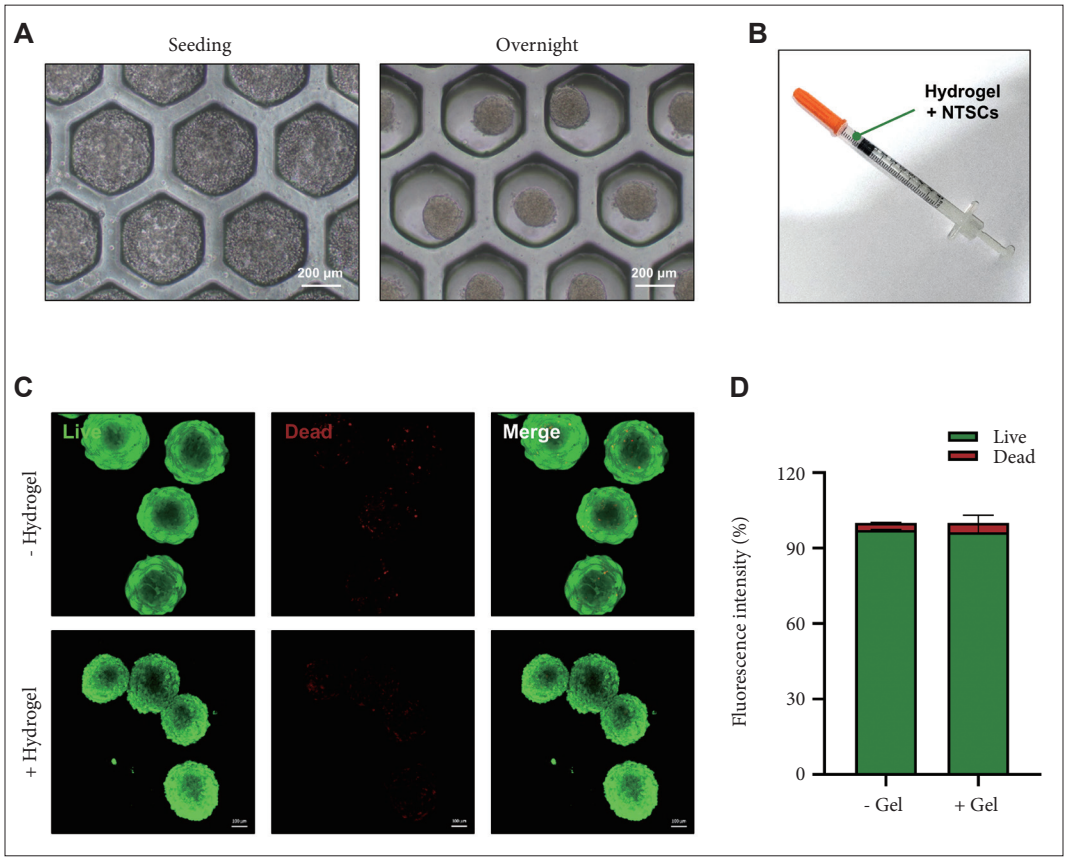

Fig. 3. Development and application of an hNTSC-based therapeutic agent. A: hNTSCs immediately after seeding into StemFIT 3D and after overnight incubation. B: Formation of an injectable therapeutic agent by mixing collagen hydrogel with hNTSC spheroids. C: Comparison of live/dead cell viability before and after mixing hNTSC spheroids with collagen hydrogel (Scale bar=100 μm). D: Quantification of live/dead cell viability. hNTSC, human nasal turbinate stem cell.

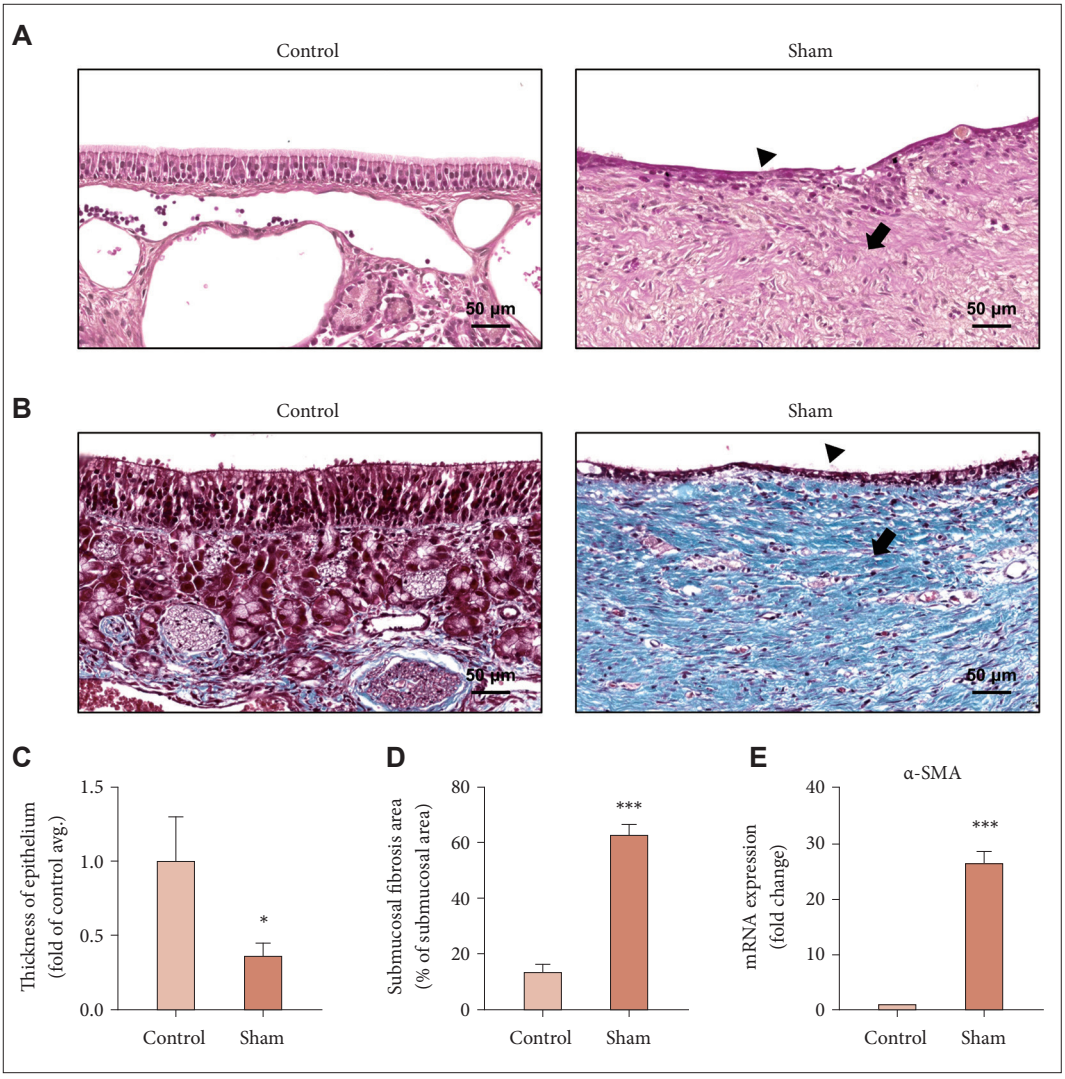

Fig. 4. Confirmation of ENS induction in the rabbit model. A and B: H&E staining (A) and MT staining (B) in control and sham groups at 400× magnification. Squamous cell metaplasia (arrowhead), fibrosis (arrow) in sham group. C and D: Quantification of epithelial thickness (p=0.024) (C) and submucosal fibrosis area (p<0.0001) (D). E: Relative α-SMA mRNA expression determined through RT-qPCR (p<0.0001). Data are presented as mean±SD, with statistical significance indicated as *p<0.05 and ***p<0.001. ENS, empty nose syndrome; H&E, hematoxylin and eosin; MT, Masson trichrome; SMA, smooth muscle actin; RT-qPCR, real-time polymerase chain reaction.

2.99% in the control group to 62.76%±3.87% (Fig. 4D). Expression of the fibrosis marker α-SMA increased by 26.43±2.23-fold compared to the control (Fig. 4E).

Evaluation of therapeutic efficacy in ENS

Histological and mRNA expression analyses of treated areas were performed one month after administration of the hNTSC-based therapeutic agent. Representative H&E-stained images from each group are shown in Fig. 5A. These images illustrate epithelial thinning and architectural disruption in the sham and vehicle groups, whereas treatment groups—particularly the medium-dose group—showed significant restoration of pseudostratified epithelium. Histological analysis demonstrated increased epithelial thickness in the treatment groups compared to the sham and vehicle groups, although this improvement did not exhibit a strictly dose-dependent response. When quantified relative to the sham group (set as 1 fold), epithelial thickness fold changes were 1.11±0.16 in the vehicle group, indicating minimal therapeutic effect. In contrast, the treatment groups showed increased fold changes: 1.37±0.46 (low dose), 3.34±1.61 (medium dose), and 1.95±0.49 (high dose). The medium-dose group (1×10^7 cells/mL) exhibited the greatest improvement (Fig. 5B). Despite marked enhancement in epithelial thickness, histological evaluation revealed that complete restoration to normal architecture was not fully achieved, though substantial regenerative changes with only

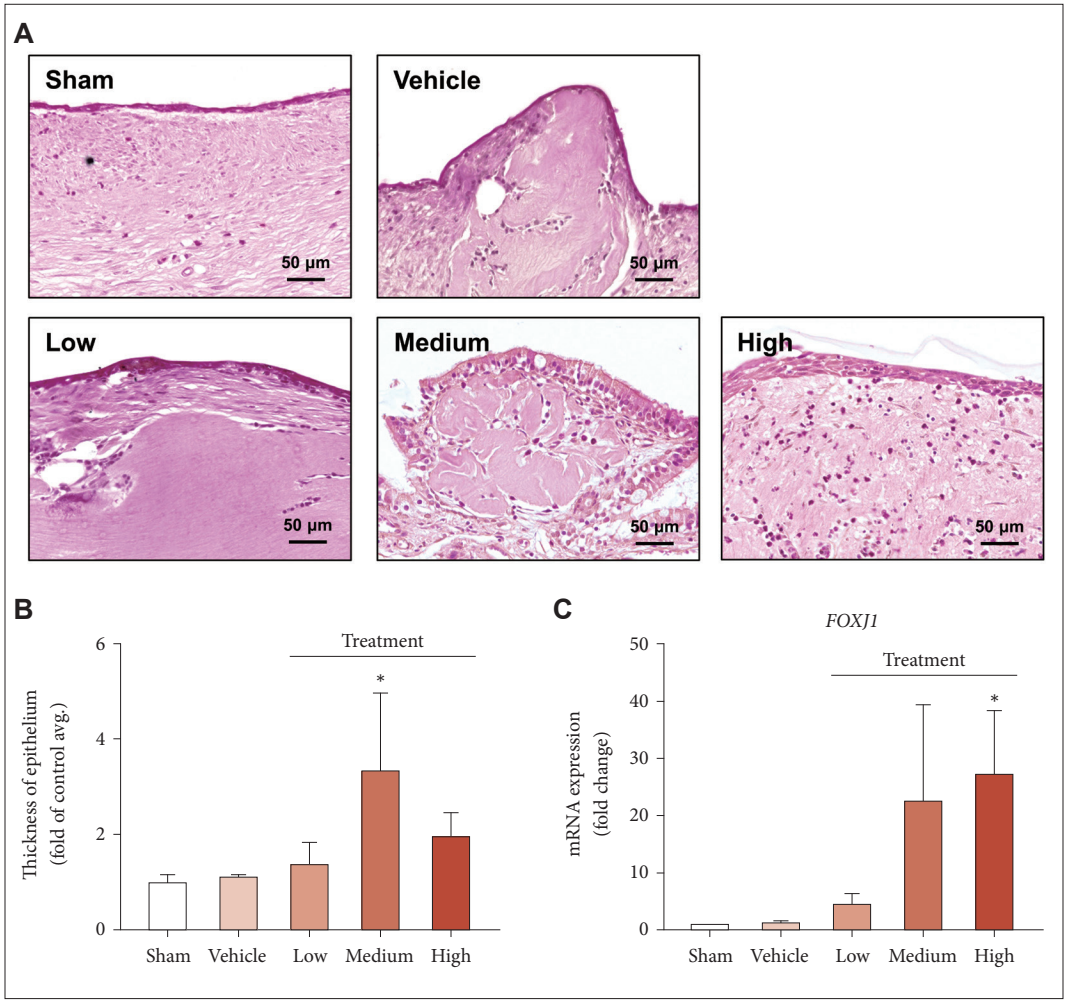

Fig. 5. Assessment of therapeutic efficacy in each group. A: Histological examination of tissue samples from sham, vehicle, and treatment groups using H&E staining at 400× magnification. B: Quantification of epithelial thickness in each group (p=0.020). C: *FOXJ1* mRNA expression levels analyzed by RT-qPCR (p=0.036). Data are presented as mean±SD, with statistical significance denoted as *p<0.05. H&E, hematoxylin and eosin; RT-qPCR, real-time quantitative polymerase chain reaction.

minor structural deviations were observed.

Similarly, mRNA expression trends reflected tissue morphology. *FOXJ1* expression levels in the vehicle group were 1.39±0.19-fold higher than in the sham group, demonstrating minimal change. However, in the treatment groups, *FOXJ1* mRNA significantly increased, with fold changes of 4.52±1.86 (low dose), 22.61±16.83 (medium dose), and 27.25±11.15 (high dose). Interestingly, unlike histological findings, *FOXJ1* expression was highest in the high-dose group (Fig. 5C).

DISCUSSION

ENS is a debilitating disease that significantly impairs patients' quality of life, causing persistent nasal discomfort, paradoxical nasal obstruction, dyspnea, and psychological distress [20]. Despite anatomically open nasal airways, patients experience sensations of suffocation due to impaired neurosensory feedback, disrupted nasal aerodynamics, and mucosal atrophy [21]. These pathophysiological changes contribute to the chronic nature of ENS and make effective treatment challenging. Conservative treatments, such as nasal humidification, saline irrigation, and intranasal medications, provide only limited symptom relief, whereas surgical interventions, including implant-based reconstruction, yield inconsistent outcomes [22]. Given the absence of universally effective treatments, innovative regenerative approaches are urgently required. Recent advances in cell-based therapies have demonstrated promise in regenerating damaged tissues in various refractory conditions, including ENS [21,23].

In this study, we investigated the therapeutic potential of hNTSCs combined with collagen hydrogel in a rabbit ENS model. Medium-dose hNTSC treatment (1×10^7 cells/mL) sig-

nificantly increased epithelial thickness, indicating optimal regenerative effects. Higher doses led to increased *FOXJ1* expression but did not result in superior histological recovery. This finding emphasizes the critical importance of precise dose optimization in stem cell therapies for ENS. Excessive cell concentrations may disrupt cellular interactions and alter microenvironmental conditions, potentially diminishing therapeutic efficacy.

hNTSCs have attracted attention as a promising source for regenerative medicine due to their strong proliferative capacity, immunomodulatory properties, and ability to secrete trophic factors promoting tissue repair. Compared to other stem cell types, hNTSCs are easily harvested from nasal turbinate tissue, mitigating ethical concerns associated with embryonic or induced pluripotent stem cells [23]. Their capacity to enhance epithelial regeneration, support ciliary function, and modulate local inflammation makes them particularly suitable for ENS treatment. Additionally, combining hNTSCs with biomaterials such as collagen hydrogel may enhance cell survival, integration, and therapeutic efficacy by providing a supportive microenvironment. Our findings suggest that hNTSC-based therapy represents a viable regenerative strategy for ENS, addressing the critical need for effective treatment options.

Cell-based therapies have shown promising results for treating refractory diseases, but therapeutic efficacy varies considerably depending on cell concentration, form, and incorporation with biomaterials. Prior studies indicate that optimal engineering of therapeutic agents can enhance cell viability, multipotency, and secretion of repair-promoting factors, thus improving therapeutic outcomes [24-26]. In this study, we aimed to determine the optimal hNTSC concentration to maximize therapeutic benefits in an ENS animal model. We administered various doses of hNTSC-based cell therapy to identify the most effective concentration for ENS treatment. Additionally, to enhance therapeutic efficacy, we combined hNTSC spheroids with collagen hydrogel at different concentrations. We evaluated potential adverse effects by assessing cell viability and found no significant difference between spheroids alone and those combined with collagen hydrogel. This result confirms the biocompatibility and safety of collagen hydrogel with hNTSCs.

In our previous studies, we successfully developed an ENS animal model using electrocautery [18]. This study aimed to verify the reproducibility of this method, confirming that electrocautery reliably induced key pathological features of ENS, including pseudostratified epithelial atrophy, squamous metaplasia, and submucosal fibrosis. The consistent demonstration of these pathological changes indicates that this model is appropriate for evaluating the efficacy of therapeutic agents.

The administration of hNTSC-based therapeutic agents at varying concentrations did not result in a strictly dose-dependent therapeutic effect on ENS, as demonstrated by histological analyses. This suggests that excessively low or high cell concentrations may not yield optimal outcomes. The medium dose of 1×10^7 cells/mL (50 μL administered volume) demonstrated the most effective therapeutic concentration, significantly improving mucosal epithelium atrophy. Although epithelial thickness showed the greatest improvement at this concentration, *FOXJ1* mRNA expression, a marker essential for ciliated cells crucial for mucosal function, was highest in the high-dose group. The elevated *FOXJ1* expression may be due to enhanced secretion of repair-associated proteins by hNTSCs, yet it did not directly correlate with histological recovery. This discrepancy suggests that *FOXJ1* expression alone may not predict functional mucosal recovery. To facilitate clinical translation, we estimated the equivalent therapeutic agent volume for humans based on anatomical differences. Considering the human nasal cavity is approximately 20-fold larger than that of rabbits, a volume of around 1 mL would maintain comparable local hNTSC concentrations.

The present study has several limitations. Notably, the small sample size (n=3 per group) may limit statistical power and generalizability. Nevertheless, this proof-of-concept study aimed primarily to identify dose-dependent trends, and consistent histological and molecular improvements were observed. Future investigations with larger sample sizes are necessary to confirm these findings conclusively.

In conclusion, this study identified the optimal hNTSC concentration for effectively treating ENS. Based on the therapeutic dose demonstrated in the animal model, this approach holds potential for clinical translation. The results of this study provide a promising therapeutic strategy for ENS, a condition currently lacking effective treatment options.

Availability of Data and Material

The datasets generated and analyzed during the current study are available from the corresponding author upon reasonable request.

Conflicts of Interest

Yun Jin Kang and Do Hyun Kim who are on the editorial board of the *Journal of Rhinology* were not involved in the editorial evaluation or decision to publish this article. All remaining authors have declared no conflicts of interest.

Author Contributions

Conceptualization: Yun Jin Kang. **Data curation:** Yun Jin Kang, Dan Bi Park. **Formal analysis:** Dan Bi Park. **Funding acquisition:** Do Hyun Kim. **Investigation:** Seung Yeon Yoo, Sung Won Kim. **Methodology:** Dan Bi Park. **Project administration:** Sung Won Kim, Do Hyun Kim. **Resources:** Dan Bi Park. **Software:** Dan Bi Park. **Supervision:** Sung Won Kim, Do Hyun Kim. **Validation:** David W. Jang, Mi Hyun Lim. **Visualization:** Dan Bi Park, Jae Yoon Lee. **Writing—original draft:** Yun Jin Kang, Dan Bi Park. **Writing—review & editing:** Yun Jin Kang, Dan Bi Park.

ORCID iDs

Yun Jin Kang https://orcid.org/0000-0002-7677-4219
Dan Bi Park https://orcid.org/0009-0006-1223-9141
David W. Jang https://orcid.org/0000-0003-4200-7174
Mi Hyun Lim https://orcid.org/0009-0009-7576-5247
Jae Yoon Lee https://orcid.org/0000-0003-4973-0859
Seung Yeon Yoo https://orcid.org/0000-0002-7713-2103
Sung Won Kim https://orcid.org/0000-0002-8981-2536
Do Hyun Kim https://orcid.org/0000-0002-9248-5572

Funding Statement

This research was supported by the Korean Fund for Regenerative Medicine, funded by the Korean government (No. 23C0121L1).

Acknowledgments

None

REFERENCES

1) Kim DH, Hwang SH. A review of the long-term efficacy of submucosal medpor implantation for empty nose syndrome: a short communication. J Rhinol 2024;31(3):176-8.
2) Sozansky J, Houser SM. Pathophysiology of empty nose syndrome. Laryngoscope 2015;125(1):70-4.
3) Scheithauer MO. Surgery of the turbinates and "empty nose" syndrome. GMS Curr Top Otorhinolaryngol Head Neck Surg 2010;9:Doc03.
4) Kimbell JS, Frank DO, Laud P, Garcia GJ, Rhee JS. Changes in nasal airflow and heat transfer correlate with symptom improvement after surgery for nasal obstruction. J Biomech 2013;46(15):2634-43.
5) Esteban-Ortega F, Rosique-López L, Ochoa-Ríos JA, Rodríguez-Romero R, Burgos-Olmos MA. Empty nose syndrome: new insights from a CFD approach. Eur Arch Otorhinolaryngol 2025;282(3):1319-26.
6) Balakin BV, Farbu E, Kosinski P. Aerodynamic evaluation of the empty nose syndrome by means of computational fluid dynamics. Comput Methods Biomech Biomed Engin 2017;20(14):1554-61.
7) Scolding NJ, Pasquini M, Reingold SC, Cohen JA; International Conference on Cell-Based Therapies for Multiple Sclerosis. Cell-based therapeutic strategies for multiple sclerosis. Brain 2017;140(11):2776-96.
8) Maron-Gutierrez T, Laffey JG, Pelosi P, Rocco PR. Cell-based therapies for the acute respiratory distress syndrome. Curr Opin Crit Care 2014;20(1):122-31.
9) Hoang DM, Pham PT, Bach TQ, Ngo ATL, Nguyen QT, Phan TTK, et al. Stem cell-based therapy for human diseases. Signal Transduct Target Ther 2022;7(1):272.
10) Vangsness CT Jr, Farr J 2nd, Boyd J, Dellaero DT, Mills CR, LeRoux-Williams M. Adult human mesenchymal stem cells delivered via intra-articular injection to the knee following partial medial meniscectomy: a randomized, double-blind, controlled study. J Bone Joint Surg Am 2014;96(2):90-8.
11) Jo CH, Chai JW, Jeong EC, Oh S, Shin JS, Shim H, et al. Intra-articular injection of mesenchymal stem cells for the treatment of osteoarthritis of the knee: a 2-year follow-up study. Am J Sports Med 2017;45(12):2774-83.
12) Lee NH, Bayaraa O, Zechu Z, Kim HS. Biomaterials-assisted spheroid engineering for regenerative therapy. BMB Rep 2021;54(7):356-67.
13) Ohori-Morita Y, Niibe K, Limraksasin P, Nattasit P, Miao X, Yamada M, et al. Novel mesenchymal stem cell spheroids with enhanced stem cell characteristics and bone regeneration ability. Stem Cells Transl Med 2022;11(4):434-49.
14) Griffin KH, Fok SW, Kent Leach J. Strategies to capitalize on cell spheroid therapeutic potential for tissue repair and disease modeling. NPJ Regen Med 2022;7(1):70.
15) Pangjantuk A, Kaokaen P, Kunhorm P, Chaicharoenaudomrung N, Noisa P. 3D culture of alginate-hyaluronic acid hydrogel supports the stemness of human mesenchymal stem cells. Sci Rep 2024;14(1):4436.
16) Liu L, Chen S, Song Y, Cui L, Chen Y, Xia J, et al. Hydrogels empowered mesenchymal stem cells and the derived exosomes for regenerative medicine in age-related musculoskeletal diseases. Pharmacol Res 2025;213:107618.
17) Li B, Zhang L, Yin Y, Chen A, Seo BR, Lou J, et al. Stiff hydrogel encapsulation retains mesenchymal stem cell stemness for regenerative medicine. Matter 2024;7(10):3447-68.
18) Park DB, Lee JY, Kim SW, Kim DH. Tissue specific stem cell therapy for airway regeneration. Cell Prolif 2024;57(10):e13662.
19) Lamo-Espinosa JM, Mora G, Blanco JF, Granero-Moltó F, Nuñez-Córdoba JM, Sánchez-Echenique C, et al. Intra-articular injection of two different doses of autologous bone marrow mesenchymal stem cells versus hyaluronic acid in the treatment of knee osteoarthritis: multicenter randomized controlled clinical trial (phase I/II). J Transl Med 2016;14(1):246.
20) Kim DH, Basurrah MA, Kim SW, Kim SW. Surgical and regenerative treatment options for empty nose syndrome: a systematic review. Clin Exp Otorhinolaryngol 2024;17(3):241-52.
21) Kim DH, Kim SW, Basurrah MA, Hwang SH. Evaluation of post-intervention outcomes in patients with empty nose syndrome. Laryngoscope 2024;134(5):2005-11.
22) Dholakia SS, Yang A, Kim D, Borchard NA, Chang MT, Khanwalkar A, et al. Long-term outcomes of inferior meatus augmentation procedure to treat empty nose syndrome. Laryngoscope 2021;131(11):E2736-41.
23) Kim DH, Hwang SH. Human nasal turbinate-derived stem cells for tissue engineering and regenerative medicine. J Rhinol 2024;31(3):133-7.
24) Kharbikar BN, Mohindra P, Desai TA. Biomaterials to enhance stem cell transplantation. Cell Stem Cell 2022;29(5):692-721.
25) Vorwald CE, Ho SS, Whitehead J, Leach JK. High-throughput formation of mesenchymal stem cell spheroids and entrapment in alginate hydrogels. Methods Mol Biol 2018;1758:139-49.
26) Nilforoushzadeh MA, Khodadadi Yazdi M, Baradaran Ghavami S, Farokhimanesh S, Mohammadi Amirabad L, Zarrintaj P, et al. Mesenchymal stem cell spheroids embedded in an injectable thermosensitive hydrogel: an in situ drug formation platform for accelerated wound healing. ACS Biomater Sci Eng 2020;6(9):5096-109.